HYDROTHERMAL SYNTHESIS OF TiO$_2$-Al$_2$O$_3$-CARBON NANOTUBE NANOCOMPOSITE AND ITS CHARACTERIZATION

by

NUR ALYAA BALQIS BINTI AZMI

A report submitted in fulfilment of the requirements for the degree of

Bachelor of Applied Science (Materials Technology) with Honours

FACULTY OF EARTH SCIENCES UNIVERSITY MALAYSIA KELANTAN

2017

DECLARATION

I declare that this thesis entitled "Hydrothermal Synthesis of TiO_2-Al_2O_3-Carbon nanotube Nanocomposite and its Characterization" is the result of my own research except as cited in the references. The thesis has not been accepted for any degree and is not concurrently submitted in candidature of any other degree.

_____

Name : Nur Alyaa Balqis binti Azmi

Date :

ACKNOWLEDGEMENT

Final Year Project (FYP) is a program to give an opportunity for students to be to conduct a research. From the beginning, I have been supported by many people. This is the opportunity for me to express my gratitude to them.

Firstly I would like to express my appreciation to my supervisor, Dr. Mahani binti Yusoff for guiding me during the preparation of this project. She has been very attentive towards me and gave me a lot of information about this project in order to complete this project. Thank you for being patient in responding toward reinforcing view. Then, I am also grateful toward my co-supervisor Dr. Nik Raihan binti Nik Yusof.

Then, I also wanted to say to thank you the Faculty of Earth Science for giving me an opportunity to experience many things through this project. Furthermore, I also have been provided with complete instruments that have helps me in complete my study. I am also grateful to UMK staff for helping me in running the experiment.

I would also like to thanks my fellow friends (Farihah and Huda) for creating fun environment. Besides that, I would also like to thank my parents for supporting and encouraging me in completing this project. Thank you.

HYDROTHERMAL SYNTHESIS OF TiO$_2$-Al$_2$O$_3$-CARBON NANOTUBENANOCOMPOSITE AND ITS CHARACTERIZATION

ABSTRACT

In this study, the TiO$_2$-Al$_2$O$_3$-CNT nanocomposite was successfully synthesized via hydrothermal method for 24 hours at 200ºC. Nanocomposites were characterized by X-ray Diffraction (XRD), Fourier Transformation Infrared Spectrophotometer (FTIR), Optical Microscope (OM) and UV-Vis. The results showed that the major peaks visible in all patterns were identified as anatase TiO$_2$ with the absence of rutile. Hydrothermal induced no new face formation but only altered TiO$_2$ structure. Agglomerated of TiO$_2$, Al$_2$O$_3$ and CNT particles were observed in nanocomposite. The highest photocatalytic aktivity of methyl orange was achieved by nanocomposite with no addition of CNT.

HIDROTERMA SINTESIS TiO$_2$-Al$_2$O$_3$-CARBON NANOTUBE NANOKOMPOSIT DAN PENCIRIANNYA

ABSTRAK

Dalam kajian ini, nanokomposit TiO$_2$-Al$_2$O$_3$-CNT telah berjaya disintesis melalui kaedah hidroterma selama 24 jam pada suhu 200ºC. Nanokomposit telah dicirikan menggunakan Pembelauan sinar-X (XRD), Transformasi Fourier Inframerah Spektrofotometer (FTIR), Mikroskop Optik (OM) dan UV-Vis. Hasil kajian menunjukkan bahawa puncak utama boleh dilihat dalam semua corak dikenal pasti sebagai anatase TiO$_2$ tanpa kehadiran rutil. Hidroterma juga menyebabkan tiada pembentukan fasa baru tetapi hanya mengubah struktur TiO$_2$. Partikel gumpalan TiO$_2$, Al$_2$O$_3$ dan CNT diperhatikan dalam nanokomposit. Kuantiti tetinggi aktiviti fotokatalitik metil jingga dicapai oleh nanokomposit tanpa penambahan CNT.

TABLE OF CONTENTS

CHAPTER 4: RESULTS AND DISCUSSION

CHAPTER 5: CONCLUSION

LIST OF TABLES

viii

CHAPTER 1

INTRODUCTION

1.1 Background of Study

Titania (TiO_2) is one of the types of large band gap (3.2 eV) semiconductor materials with unique properties, such as having a low toxicity, low cost, high stability and superior photocatalytic activity. Moreover, TiO_2 also have been attracted an intensive attention in an environmental pollution control. Recently research on TiO_2 nanotube is mainly focused on the understanding of its strong photocatalytic activity which is useful in environmental pollution remediation and water purification (Qamar, 2008; Sekabira *et al*., 2010). Furthermore, TiO_2 has sufficient band gap energies for specially promoting or catalyzing a wide range of chemical reactions of environmental interest (Ismael *et al*., 2007). It is also have been used to oxidize the industrial pollutants and it is converted into the products like H_2O, alcohols and other useful hydrocarbons. This material is also one of the most promising photocatalyst materials.

The presence of the pollutants such as CO_2, NO_2 in the air, organic dyes (methyl orange) and many other organic hydrocarbons such as phenol, formaldehyde and gasoline which contribute to produce many industrial processes such as manufacture of dyes, food processing, pesticides and polymers in industrial wastes. It also may cause severe environmental problems (Chein and Shih, 2007; Ismael *et al*., 2007; Qamar, 2008).

1

TiO$_2$ also absorb UV light a chain of the events which possibly leading to the production of radicals. According to Khalid *et al*., (2012), the characteristics of composite catalyst must have stronger light absorption in visible light region and it is also showed excellent photocatalytic activity. However, pure TiO$_2$ under visible light irradiation for degradation is limited. Therefore, a surface modification of TiO$_2$ can be made to improve the photocatalytic activities which can alter the mechanism and accelerate the kinetics of photocatalysis. There have been many attempts to enhance the photocatalytic activity of TiO$_2$ using various metallic and non- metallic dopants. It is also not for only narrowing the band gap but also provide benefits toward photo-generated electron-hole separation.

In this study, nanocomposite material is a matrix which nanoparticle has been added in order to improve a particular property of a material. Ceramic-matrix nanocomposites are popular which their chemical compound is from the group of oxides, nitrides, borides and sillicates. The example is alumina or aluminium oxides (Al$_2$O$_3$), it is the most widely uses matrix in order to produce composite due to its high thermal conductivity, melting point and thermal expansion. Therefore, it is possible making for high temperature application (Trunec *et al*., 2015). Al$_2$O$_3$ also has been used as a dopant in TiO$_2$ nanocomposite. Al$_2$O$_3$ is choose to be doped with TiO$_2$ is due to its properties which is relatively high thermal conductivity, electrical, insulators and it is also an amphotheric substance that can react with other acid and bases.

Recently, carbon based nanomaterials, such as carbon nanotube (CNTs) and graphene, have been used as the hybrid component in TiO$_2$. This also due to their unique electrical properties, superior chemical stability and good conductor. CNTs

are carbon based fillers which is commonly used in nanocomposite research in order to improved structural and functional properties of the host materials. It is also have increase the number of studies over the past decade seeking to develop carbon nanotube-titania (CNT-TiO$_2$) mixtures or composites with enhanced photocatalytic activity. This material also possesses the stiffest and the strongest properties among the materials that ever found as stated by Long *et al*., (2015).

Hydrothermal method has been widely used to prepare TiO$_2$ doping nanocomposite due to its low cost and able to narrow the band gap (Leary and Westwood, 2011). This method also involves the synthesis of nanocomposite from aqueous solution in an autoclave with the presence of high temperature and pressure. Furthermore, this method can be simple and facile (Chang *et al*., 2012) and eco-friendly (Ezeigwe *et al*., 2015). The production of TiO$_2$ nanocomposite by hydrothermal method contributed more uniform distribution of particles and less agglomeration compared to the sol-gel method. Moreover, it is also one of the methods that use to synthesize ceramic based composites.

Photocatalytic reaction can be defined as a reaction induced by photoabsorption of a solid material, the photocatalyst which remains unchanged during the reaction. Semiconductor photocatalysis is broadly known as the catalysis of a photochemical reaction at the surface of the solid semiconductor. However, according to Ohtani *et al*., (2008), not all photocatalytic processes can be classed as catalytic. Catalysis refers to the acceleration of an energetically downhill reaction by the reduction of the activation energy, where the photocatalysis includes reactions which proceed energetically uphill and accumulating energy such as water splitting. In the semiconductor, titania (TiO$_2$) photocatalysis usually introduced with respect to

3

a band model, where there must be at least two reactions that will be occurring simultaneously. These processes also must occur at the equal rates if photocatalyst is to remain unchanged.

The aim of this study is to produce TiO_2 - Al_2O_3 - CNT nanocomposite using hydrothermal method. The performance of this nanocomposite on photocatalytic activity of methyl orange (MO) will also be discussed.

1.2 Problem Statement

TiO_2 has large band gap (3.2 eV) which only effective under ultra-violet (UV) range and less effective in visible light. In order to make it reacts with molecule of dye under visible light, the band gap of TiO_2 must be narrowed. This can be achieved by doping either with metal, non-metal or hybrid materials. The current research shows that the use of TiO_2 - Al_2O_3 is not widely applied for the study of photocatalytic in waste water application. Moreover, addition of carbon nanotube in TiO_2 photocatalyst nanocomposite may help to increase photocatalytic capability under visible light.

1.3 Objectives

The objectives of this research are:

1) To hydrothermal synthesized of TiO_2 - Al_2O_3 - CNT nanocomposite using hydrothermal method.

2) To investigate the photocatalytic activity of methyl orange using hydrothermally synthesized TiO_2 - Al_2O_3 - CNT nanocomposite.

1.4 Expected Outcomes

TiO$_2$ - Al$_2$O$_3$ - CNT nanocomposite is expected to have small band gap energy compared to that pure TiO$_2$ for photocatalytic degradation of methyl orange. The effect of different compositions of Al$_2$O$_3$ and CNT during hydrothermal treatment on TiO$_2$ - Al$_2$O$_3$ - CNT can be distinguished.

CHAPTER 2

LITERATURE REVIEW

2.1 Nanopaticle Titania (TiO$_2$)

Titania (TiO$_2$) is one type of semiconductor materials with unique properties, where the materials have low toxicity, low cost, high stability and superior photocatalytic activity. In nanoscale, this material is also one of the most promising photocatalyst (Jiang *et al*., 2012; Khalid *et al*., 2012; Poliah *et al*., 2011; Park *et al*., 2013).

According to Khalid *et al*., (2012), TiO$_2$ also consists of three different types of crystallographic form which are anatase, rutile and brookite. Pure anatase TiO$_2$ possesses wide band gap (3.2 eV). Figure 2.1 shows the crystallographic form of TiO$_2$. There are many factors including the phase composition, crystallite size, morphology, specific surface area and energy band gap and so on that can influence the photocatalytic activity of TiO$_2$. Besides, TiO$_2$ also has various types of morphologies such as spheres, hollow spheres, nanotubes and nanowires (Figure 2.4).
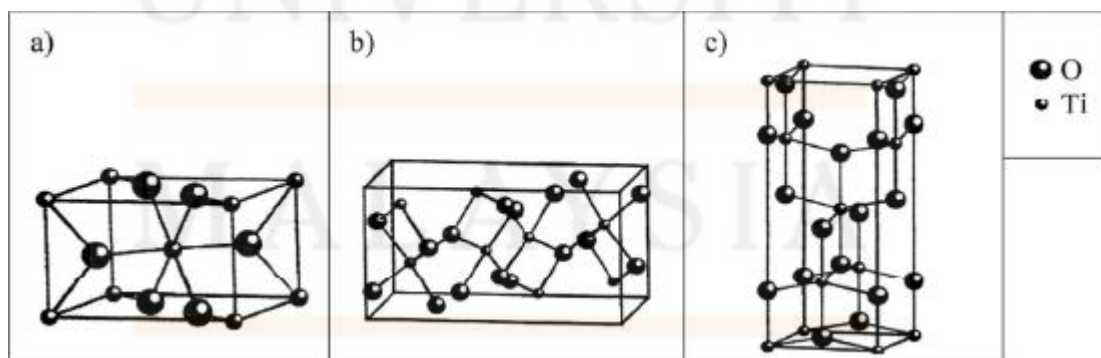
Figure 2.1: Crystallographic form of TiO$_2$; a) Rutile: b) Brookite: c) Anatase (Bagheri *et al*., 2015).

6
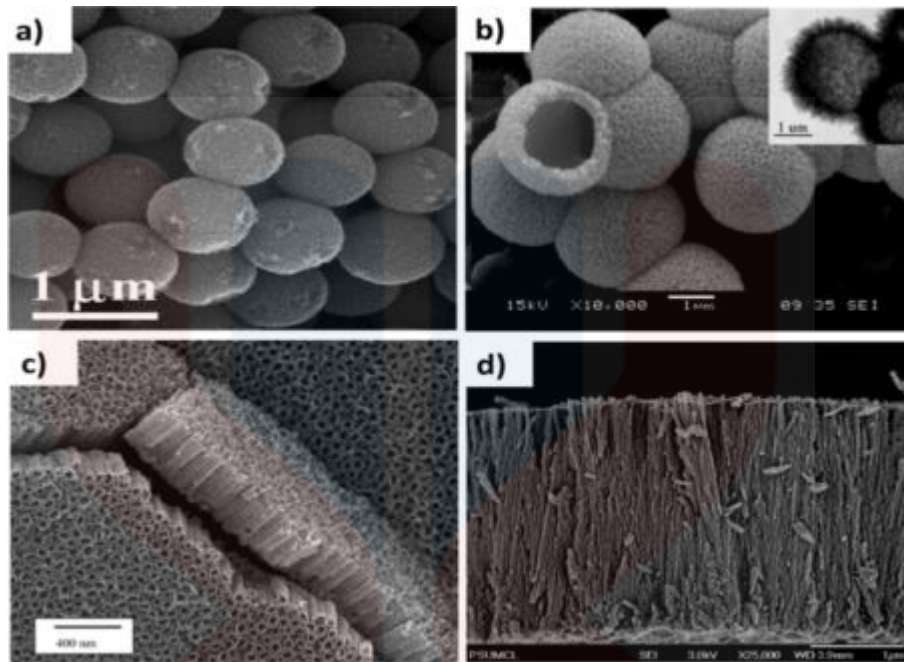
Figure 2.2: SEM images of TiO_2 with various morphologies: (a) spheres, (b) hollow spheres, (c) nanotubes, (d) nanowires (Nursam *et al.*, 2015).

It is important to study the relationship between the phase composition and the photocatalytic activity of TiO_2 under different synthesis conditions. Moreover, this material is extensively explored as a catalyst for the water splitting and for the production of solar hydrogen (Chen *et al.*, 2005). As a catalyst for the conversion of the greenhouse gases into the energy that produced the products for methane and methanol (Chen *et al.*, 2005; Khan *et al.*, 2006). Hussain and Siddiqa, (2011) also stated that the nanotubes are widely exploited into the lithium ions batteries, electrochemical devices, gas sensors, photoluminescence ion exchange and in photovoltaic dye sensitized solar cells.

The photocatalytic activity of TiO_2 is initiated by the absorption of the photon hv_1 with energy equal to the band gap of TiO_2 by producing an electron-hole pair on the surface of TiO_2 nanoparticle as the schematized in Figure 2.3 (Zaleska, 2008). An electron is promoted to the conduction band (CB) and the positive holes are formed

7

in the valance band (VB). The excited-state electrons and hole will be recombined and dissipate the input energy as the heat is trapped in the metastable surface states, or it will react with the electron donor and acceptor which will be absorbed on the semiconductor surface. Then, after it reacts with water, the holes will produce hydroxyl radical with high redox oxidizing potential. Depending on the condition, the holes, OH radicals, O_2^-, H_2O and O_2 will play the important roles of the photocatalytic reaction.
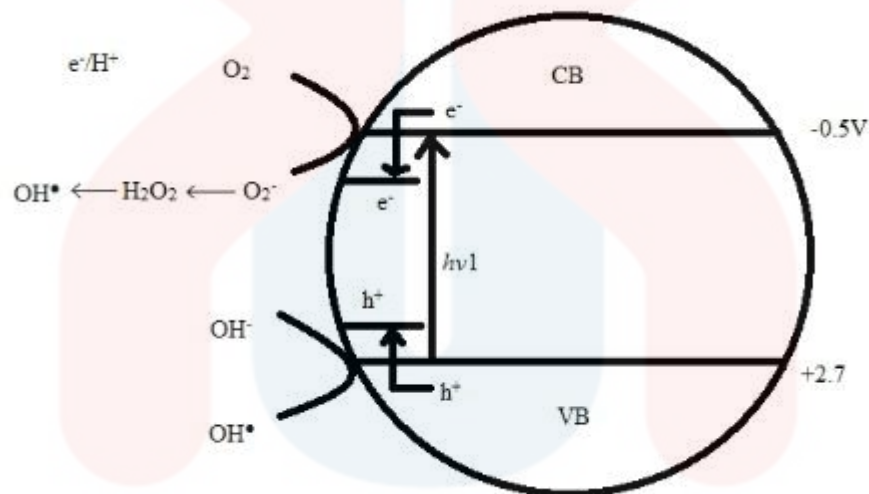
Figure 2.3: Mechanism of TiO_2 photocatalysis: hv_1: pure TiO_2 (Zaleska, 2008).

2.2 Reduction of TiO_2 nanocomposite band gap

TiO_2 possesses wide band gap (3.2 eV) which limits its uses as photocatalyst and also difficult to be recoverable because of its tiny particles. The primary purposes of incorporation of TiO_2 nanocomposite are to retard the fast charge recombination and enable the visible light absorption by creating defect states in the band gaps in the former cases, the conduction band (CB) electrons or valance band (VB) to defect states (intraband states or midgap level) or from defect states to CB

8

are allowed under sub-bandgap irradiation. Thus, TiO_2 also can be doped with other material. Usually dopant can be classified into metal ions (transition metals and noble metals) and non-metal ions, and the selection of dopant is very crucial in order to determine the overall photocatalytic activities (Park *et al*., 2013).

A significant drawback in the application of pure TiO_2 is its wide band gap which requires the use if UV light during the photocatalytic reactions thus limiting the possibility of employing the solar light. Furthermore, TiO_2 show high reactivity and chemical stability under ultraviolet light which its wavelength is less than 387nm whose the energy have exceed the band gap of 3.2 eV in the anatase phase. The development of photocatalyst exhibiting high reactivity under the visible light which is the wavelength is more than 400 nm (Zaleska, 2008).

Therefore, modifying the photocatalytic activity of metal oxide into the visible light region may require the incorporation of metal or non-metal ion would be proposed.

2.2.1 Doping with metal

The purpose of metal doping to TiO_2 nanocomposite is to increase the visible light adsorption by reducing the band gap. The most common metal dopant used for TiO_2 nanocomposite is transition metal such as Ag, Au, Cr, Fe, Mn and V (Vu *et al*., 2010).

Moreover, metal doping not only produce narrow band gap but also provide benefits toward photo-generated electron-hole separation. According to Liu *et al*., (2014) after doping Cr^{3+} into TiO_2 nanotube (TNTs), the band gap was reduced from 3.3eV to 2.3 eV. According to Zaleska (2008), the visible light photoactivity of

9

metal-doped TiO_2 can be explained by the new energy level in the band gap of TiO_2 by dispersion of metal nanoparticle in the matrix as shown in Figure 2.4. Electron is excited from defect state to the conduction band by photon energy which equal to hv_2. Besides, there are benefits of doping TiO_2 with transition metal, and it is to improve trapping of electrons to inhibit electron-hole recombination during irradiation. It also decreases the charge carrier recombination results in an enhanced photoactivity.
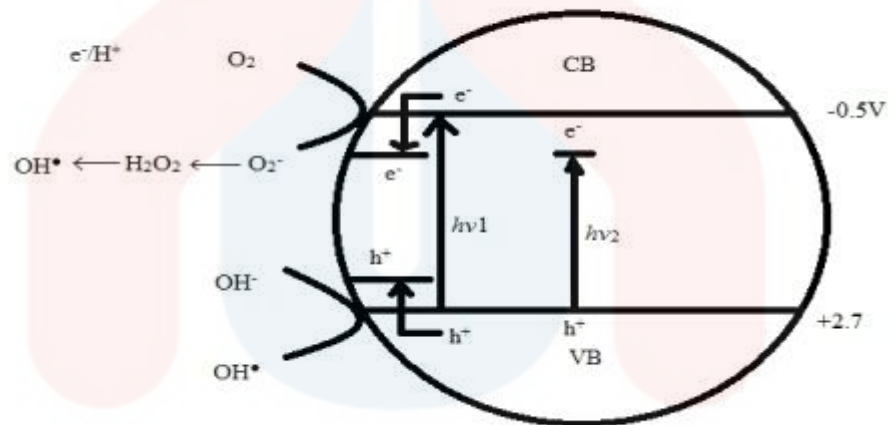
Figure 2.4: Mechanism of TiO_2 photocatalysis: hv_1: pure TiO_2; hv_2: metal doped TiO_2 (Zaleska, 2008).

2.2.2 Doping with non-metal

Recent research stated that doping with non-metal atoms such as C, S and N have received wide attention. It can be enhanced the photo-degradation of methyl orange. Moreover, Liu *et al*., (2014) stated that non-metal materials promote the generation of oxygen vacancies which provide the formation of the active sites for photocatalytic reaction. However, decreasing content of dopant reduced the photoactivity under visible light. This has been proved by Liu *et al*., (2014) that low

10

content of N dopant will result in the variation of band gap as-synthesized N-doped TiO$_2$ from 1.55 to 2.95 eV, to reduce photoactivity under visible light.

Besides, there are three main different opinion of mechanism of TiO$_2$ doped with non-metal which proved by Zaleska (2008) (Figure 2.5). First, the band gap narrowing where the anatase TiO$_2$ is doped with nitrogen because of their energy is very close, hence, the band gap of N-TiO$_2$ is narrowed. Therefore, it is able to absorb the visible light. The second is their impurity energy level, where the oxygen site of TiO$_2$ is substituted by nitrogen atom will form isolated impurity energy levels above the valance band.

Therefore, the irradiation with the UV light will excite the electron in both VB and impurity energy level. However, the illumination with visible light will only excites the electron in the impurities energy level. The third opinion is about its oxygen vacancies.
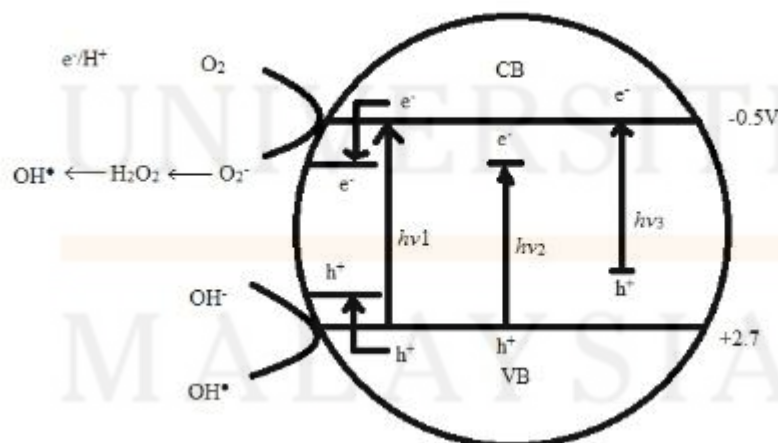
Figure 2.5: Mechanism of TiO$_2$ photocatalysis: hv_1: pure TiO$_2$; hv_2: metal-doped TiO$_2$ and hv_3: non-metal doped TiO$_2$ (Zaleska, 2008).

11

2.3 Alumina nanocomposite

Alumina (Al_2O_3) is one of metal oxides which possess low friction, high strength, high wear resistance and good corrosion resistance and it is widely used in biomedical application (Gutierrez-Gonzalez *et al*., 2015). The structure of Al_2O_3 has two different types of sites which are hexagonal and octahedral where its holds atoms. The hexagonal sites are the corner for atoms in the cell while the octahedral sites present between two layers of vertical stacking. Aluminium cations are in the 2/3 of octahedral sites and oxygen anions are in the 1/3 of octahedral sites. Therefore, each of the oxygen is shared between four octahedral. The presence of oxygen have contributes to strong bonding and gives rise to the characteristics of alumina properties (Davis, 2010).

Furthermore, Al_2O_3-based nanocomposite material has potential in technological and application. According to Davis, (2010), more than 90% of Al_2O_3 is produced in worldwide. This is due to the naturally converting bauxite into the Al_2O_3. The applications of Al_2O_3 can be found such as insulating material, electronic devices and mechanical ceramics.

According to Pei *et al*., (2014), the studies of the catalytic effect of Fe^{3+} modified the nanometer TiO_2 loaded on Al_2O_3 gives the results that proved the best photocatalytic effect can be achieved with 10% of TiO_2 composite which making the degradation are 0.71%, 3.9%,1.3% and 15.1% larger than unloaded TiO_2. Figure 2.6 shows the SEM images of TiO_2-Al_2O_3 composite.
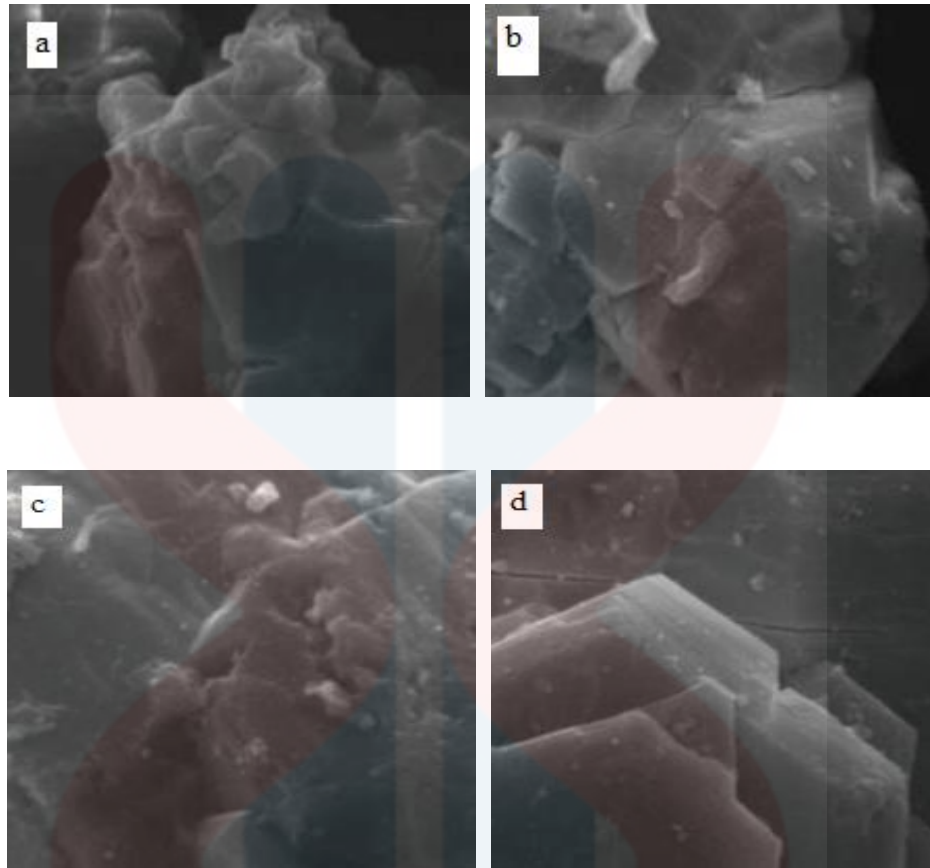
Figure 2.6: SEM images of TiO_2-Al_2O_3 composites; (a) Al_2O_3 calcining sample, (b) magnified pattern of Al_2O_3 loaded with TiO_2, (c) Al_2O_3 loaded with 10% TiO_2, (d) Al_2O_3 loaded with 5% TiO_2 (Pei *et al.*, 2014).

2.4 Carbon nanotube nanocomposite

The materials that usually have been used as reinforced materials are silicon nitrides (SiN), carbon nanotubes (CNT) and graphene and in this study, CNT is choosen as the reinforcement. Long *et al.,* (2015) stated that this material has possesses the stiffest and the strongest material that ever found. CNT is carbon-based fillers which used to improve the structural and functional properties of the host materials. Figure 2.7 shows the structure of CNT. These materials can be divided into two categories which are single wall CNT (SWCNT) and multi wall CNT (MWCNT). Figure 2.9 shows the structure of SWCNT and MWCNT.

13
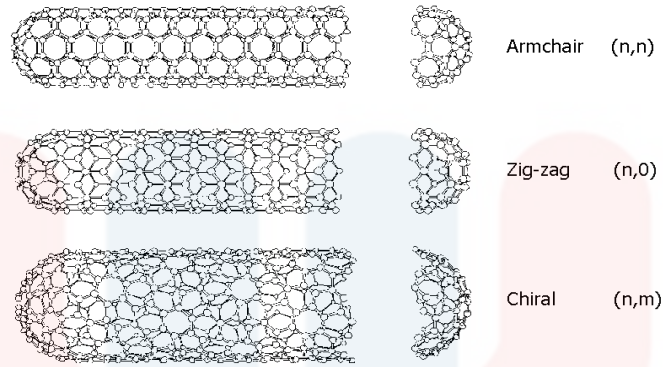
Figure 2.7: Carbon Nanotubes (CNTs) (Baksi & Biswas, 2014).
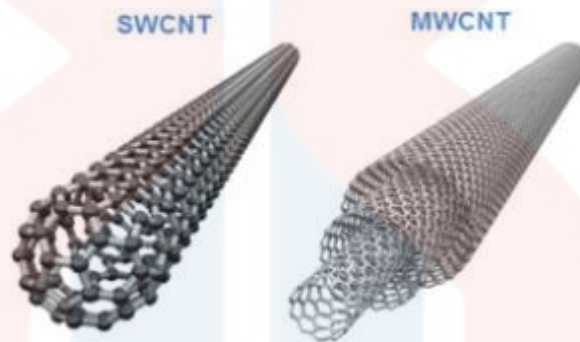
Figure 2.8: The structure of SWCNT and MWCNT (Cividanes *et al.*, 2014).

Woan *et al.*, (2008) proposed that the electronic-band structure of the CNT is very important for photocatalytic activity than the bond that exists between the CNT and TiO_2. It also stated that during photocatalysis, some degree of CNT oxidation is expected to be occurring, and that oxidised portions of CNTs then will initially permit defect states. Thus, allowing the enhancement of photogeneration of electron–hole pairs.

According to Leary and Westwood (2011), although the CNT-TiO_2 composites employing the MWCNTs are more common in the literature compared to those employing SWCNTs, it has been suggested that better understanding of the

14

proposed mechanism may be achieved through the use of SWCNTs, since their electronic properties are better defined.

Furthermore, Leary & Westwood, (2011) has stated that the different CNT loadings have been investigated in a number of studies. In most cases of TiO_2 nanoparticles loaded onto or randomly mixed with CNTs, photocatalytic activity increased up to approximate 85 wt.% CNT, after which it decreased. However, the optimum percentage of CNT appears to be highly dependent on the morphology of the photocatalyst: for mixtures/composites of CNTs loaded onto larger TiO_2 nanoparticles or nanotubes optimal activity has been found at around 20 wt.% CNT.

Moreover, Yen *et al.* (2008) also found that approximate 20 wt.% CNT to be optimum for TiO_2 nanoparticles is loaded on CNTs. In either case, there exists a compromise between increased synergistic effect from higher CNT loadings, and insufficient amounts of TiO_2 or blockage of TiO_2 active sites. The apparently contradictory findings could be partially explained based on whether the CNT is acting as an electron sink in Figure 2.9(a) or as a photosensitizer in Figure 2.9(b) or Figure (c).
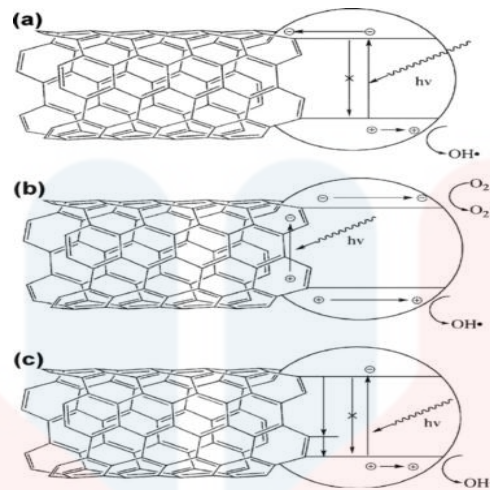
Figure 2.9: Proposed mechanisms of synergistic enhancement in TiO_2–CNT composites. (a) CNTs inhibit recombination by acting as sinks for photogenerated electrons in TiO2. (b) Photosensitizing mechanism based on electron–hole pair generation in the CNT. Depending on the relevant positions of the bands, the electron or hole may be injected into the TiO_2, generating O_2^- or OH^- species. (c) CNTs act as impurities through the Ti–O–C bonds (Leary and Westwood, 2011).

Moreover, Long *et al*., (2015) also proved that the small amout of CNT that dispersed in the copper matrix will increase the nanocomposite strength about 300% by a novel electrochemical co-deposition. Futhermore, the past research also proved that the carbon nanotubes (CNT) as a filler in Al_2O_3 matrix led to the enhancement of mechanical properties (Thomson *et al*., 2012; Estili and Sakka, 2014; Sarkar and Das, 2014).

Simoes *et al*., (2015) also proved that the aluminium matrix nanocomposites reinforced by CNT revealed an enhanced of 50% in the hardness and 200% in the tensile strength as compared with pure aluminium produced via classical powder metallurgy route.

16

2.5 Synthesis method for TiO$_2$ nanocomposite photocatalyst

2.5.1 Sol-gel method

Sol-gel method involves of dispersion of particles in liquid solution and agglomerated to produce nanoparticles. This method is used to prepare TiO$_2$ nanocomposite photocatalyst (Pei *et al*., 2014).

Moreover, this process of pure TiO$_2$ was usually derived from the reaction of hydrolysis. This process also required simplicity in controlling the doping level and particle size and it is changing the experimental conditions like hydrolysis rate, solution pH and solvent system (Sun *et al*., 2010). However, there are disadvantages for using this method. According to Carter and Norton (2013), the disadvantages of this method, are the high cost of raw materials, large volume shrinkage and cracking often happened during drying.

Furthermore, sol-gel and hydrothermal methods for the synthesis of TiO$_2$-SiO$_2$ composite nanoparticles were compared to each other and it found out that samples prepared through the hydrothermal route still possess a stable anatase phase, a large specific surface area, a small particle size, and a high photocatalytic activity even when calcined at 1000∘C. Figure 2.10 shows the typical procedure of doped-TiO$_2$ preparation by sol-gel method.
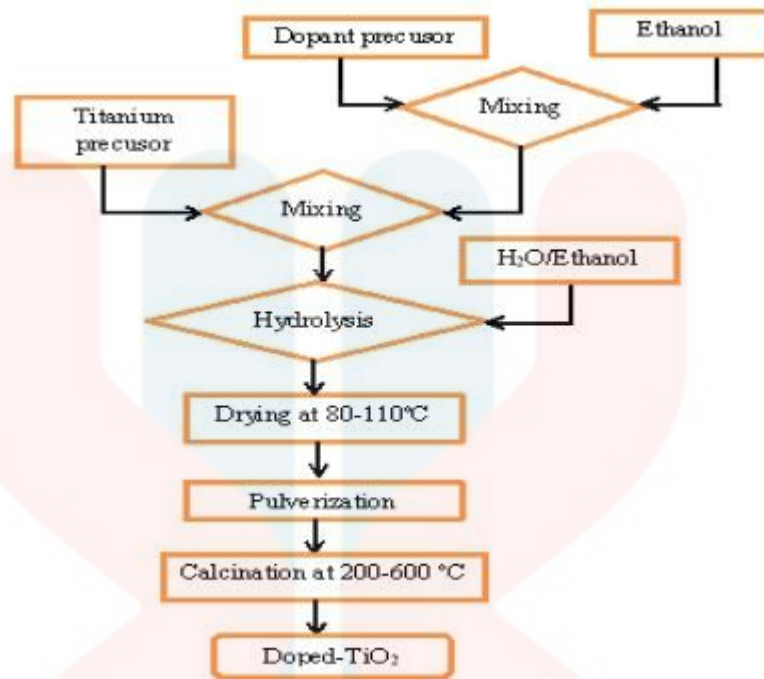
Figure 2.10: Typical procedure of doped-TiO$_2$ preparation by sol-gel method (Zaleska, 2008).

2.5.2 Hydrothermal method

Hydrothermal method involves of synthesis of nanocomposite from aqueous solution in an autoclave. Hydrothermal method is a common method to synthesis TiO$_2$ nanocomposite. TiO$_2$ is dissolved in a concentrated aqueous solution of sodium hydroxide, NaOH to form a mixture and be subjected to an autoclave. A typical hydrothermal temperature range is from 110-150 ℃. Hydrothermal synthesis is the easiest method to be operated due to its capability of large area growth of nanotube of TiO$_2$.

However, although the entire synthesis process seems to be very simple, every single step including the choice of TiO$_2$ precursors, the hydrothermal condition (temperature, the concentration of reactants, and hydrothermal duration), and the subsequent post washing procedure (washing times, acid concentration, and the sequence of washing by solvent and acid) is indeed plays the crucial role (Liu *et al*.,

2014). This has been proved by Poliah *et al*., (2011) that the hydrothermal method would be at the stable anatase phase, a large specific surface area, a small particle size, and high photocatalytic activity even it was calcined at temperature of 1000°C. Furthermore, this method has been used widely in the preparation of highly dispersed, and shape controlled such as nanotubes, nanowires and nanorods of nanocrystal TiO_2. Besides, the dopants of TiO_2 and its characteristics could be controlled by changing the physicochemical parameters of the synthesis system (Sun *et al*., 2010).

Moreover, hydrothermal synthesis is also that using temperature and pressure to produce crystal from aqueous solution usually in an autoclave. Su *et al.* (2016) stated that hydrothermal route making the synthesising process is easier due to it can control particle morphology, phase composition, particle size and microstructures of the nanocomposites. Figure 2.11 shows the HRTEM images of a single nanotube synthesized by alkali hydrothermal treatment.
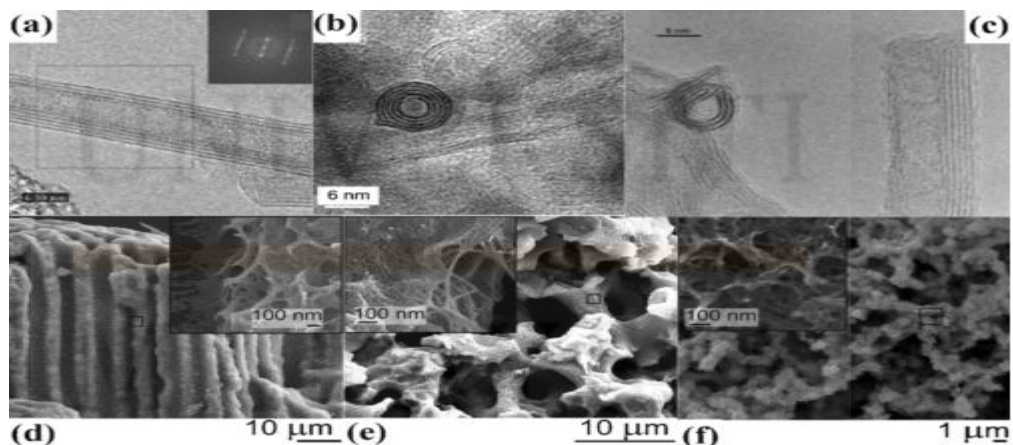
Figure 2.11: HRTEM images (a) single multi-walled nanotube; (b) cross-sections of a single TiO_2 nanotube; (c) cross-sections of a single TiO_2 nanotube; (d) TiO_2 microtubes, (e) amorphous structured TiO_2 and (f) nanotubes array (Liu *et al*., 2014).

19

2.6 Photocatalytic Activity

Photocatalysis is a reaction which uses light to activate a substance by modifying the rate of a chemical reaction without being involved itself. The photocatalyst material also must have strong oxidizing reaction with harmful substances and able to decompose the substance into carbon oxide, water and other small molecules when it is exposed to a light source. Figure 2.12 shows the photocatalytic reaction process under ultra-violet (UV) and visible light.
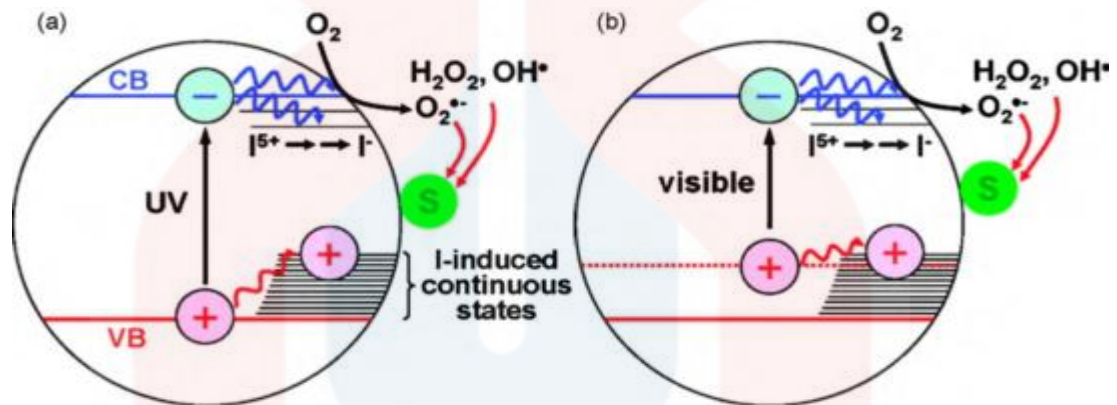
Figure 2.12: Schematic illustration of the I- TiO$_2$ photocatalytic reaction process under (a) UV irradiation and (b) visible light irradiation (Sun *et al*., 2010).

TiO$_2$ is one of the most favourable materials for photocatalyst property of semiconductors. Figure 2.13 shows the main processes in the semiconductor photocatalyst. Photocatalytic reaction may occur either in the homogeneously or heterogeneously. In the homogeneous, the catalyst and the reactants are in the same phase while the heterogeneous, the reactants and the catalyst are in the different phase. Therefore, the reaction that involves a solid photocatalyst is in the form of metal oxides or semiconductors (Nursam *et al*., 2015).

20
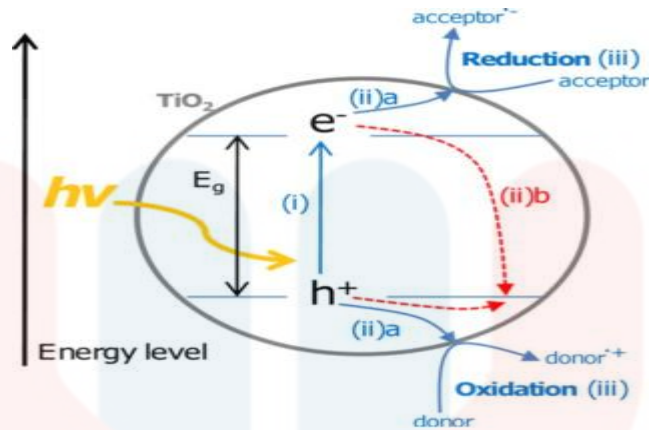
Figure 2.13: Main processes in semiconductor photocatalysis. (i) Photon absorption and electron-hole pair generation. (ii) Charge separation and migration; (ii) a to surface reaction sites or (ii) b to recombination sites. (iii) Surface chemical reaction at active sites (Leary and Westwood, 2011).

Moreover, according to Poliah *et al.*, (2011), FTIR shows the results of the sample (Ph 3) possessed high intensity of hydroxyl group. The result will also indicates that sample prepared at basic condition showed the poor MO degradation, which is in agreement with the observations. They revealed that amorphous TiO_2 has lower photocatalytic activity compared with crystalline TiO_2. Hence, SiO_2-loaded TiO_2 powder prepared under basic conditions is inefficient for high photodegradation.

CHAPTER 3

MATERIALS AND METHOD

3.1 Introduction

TiO_2 - Al_2O_3 - carbon nanotube nanocomposite were prepared using TiO_2, Al_2O_3 and carbon nanotube powders. The experimental work in this study can be divided into preparation of TiO_2 - Al_2O_3 - CNT nanocomposite using hydrothermal and its characterization. The overall work study is shown in Figure 3.1.

3.2 Raw materials

The raw materials will be used in this study are TiO_2 powder (>99.5% purity, average particle size > 21 nm) and Al_2O_3 powder (>99.9% purity, average particle size >20 μm) and carbon nanotube were purchased by Sigma Aldrich.

3.3 Preparation of TiO_2-Al_2O_3-Carbon nanotube nanocomposite

The composition of TiO_2 - Al_2O_3 - CNT were given in Table 3.1. TiO_2, Al_2O_3 and CNT will be premixed using ball milling for an hour. Then, 100 ml of 1 M of sodium hydroxide, NaOH and H_2O is added. After that, the mixture were stirred for 30 minutes and synthesized via hydrothermal method at temperatures of 200ºC for 24 hours in a sealed autoclave. Then, the sample was washed with 200 ml of 0.1 M hydrochloric acid and distilled water. The sample then was dried in an oven at 80ºC for 24 hours. Overall, research work in this study is shown in Figure 3.1.

22

```
┌─────────────────────────────────────────┐
│   TiO₂ - Al₂O₃ – CNT nanocomposite powder │
│              was prepared                 │
└─────────────────────────────────────────┘
                    │
                    ▼
┌─────────────────────────────────────────┐
│   The sample was premixes in the ball    │
│             milling for 1h               │
└─────────────────────────────────────────┘
                    │
                    ▼
┌─────────────────────────────────────────┐
│  100 ml of 1M of NaOH and H₂O were added │
│   to the mixture and stirred for 30 min  │
└─────────────────────────────────────────┘
                    │
                    ▼
┌─────────────────────────────────────────┐
│  Hydrothermal treatment at 200ºC for 24 h│
│              in autoclave                 │
└─────────────────────────────────────────┘
                    │
                    ▼
┌─────────────────────────────────────────┐
│   The sample were washed with 0.1 M of   │
│ hydrochloric acid (HCL) and distilled water│
└─────────────────────────────────────────┘
                    │
                    ▼
┌─────────────────────────────────────────┐
│  The sample were dry in the oven for 24 h │
└─────────────────────────────────────────┘
                    │
                    ▼
┌─────────────────────────────────────────┐
│       Characterization of samples         │
└─────────────────────────────────────────┘
```

The flow chart describes the following process:

1. TiO_2 - Al_2O_3 – CNT nanocomposite powder was prepared
2. The sample was premixes in the ball milling for 1h
3. 100 ml of 1M of NaOH and H_2O were added to the mixture and stirred for 30 min
4. Hydrothermal treatment at 200ºC for 24 h in autoclave
5. The sample were washed with 0.1 M of hydrochloric acid (HCL) and distilled water
6. The sample were dry in the oven for 24 h
7. Characterization of samples

Characterization of samples branches into:

- Phase identification (XRD)
- Morphology (OM)
- Photocatalytic activity
  - Photocatalytic discoloration of MO (UV-Vis)
  - Functional group (FTIR)

Figure 3.1: Overall experimental work in this research.

Table 3.1: Composition of TiO_2-Al_2O_3-CNT nanocomposite.

Nanocomposite Sample	TiO (wt %)	Al_2O_3 (wt %)	CNT (wt %)
TAC90	90	9	1
TAC80	80	19	1
TAC70	70	29	1
TAC60	60	39	1
TA50	50	50	0
T100	100	0	0

3.4 Characterization of TiO_2-Al_2O_3-Carbon nanotube nanocomposite

3.4.1 Phase identification

X-ray Diffraction (XRD) was used to determine the phase identification of TiO_2-Al_2O_3-CNT nanocomposite. The machine that was used is Bruker D2 Phaser. The step size is 0.02 º and the range of 2q angle is between 20 º to 80 º. The DIFFRAC EVA will be used for qualitative analysis.

3.4.2 Cystallite size and Internal strain

Williamson Hall method was used to calculated the crystallite size and internal strain for the TiO_2-Al_2O_3-CNT nanocomposite. In this method its needed the peak broadening. This method also needs the value of full width at half maximum which is also known as FWHM. Therefore, the graph of $B_r \cos \theta$ vs $\sin \theta$ can be

24

plotted. The crystallite size and internal strain was calculated according to the following equation:

$$\beta \cos \theta = \frac{K\lambda}{D} + 2\varepsilon \sin \theta$$

Eq.1

3.4.3 Morphologies

The optical microscope has been used to evaluate the microstrcture of TiO_2-Al_2O_3-CNT nanocomposite using metallurgical microscope model MT8100. The software that have been used by these microscope was ProGress CT3.

3.4.4 Functional group

Fourier Transformation Infrared Spectrophotometer (FTIR) was used to determine the functional group and the bonding of TiO_2-Al_2O_3-CNT nanocomposite using Nicolet IS5 Spectrometer. Thermo Scientific OMNIC Spectra software also will be used to analyse the sample. It is also used to observe the possible structure changes after doping.

3.4.5 Photocatalytic degradation of methyl orange (MO)

The performance of TiO_2-Al_2O_3-CNT nanocomposite on photocatalytic absorption of methyl orange (MO) were studied. The sample of 0.1g were added into 100 ml of 20 ppm MO dye aqueous solution. The source of visible light are provided by 500W tungsten-halogen lamp (OSRAM Germany) where 420 nm cut off filter is used to cut off the UV light to below than 420 nm. The aqueous suspension was stirred manually using a stirrer throughout this experiment. It will be subjected to the visible light irradiation start from 1 to 3 hours. At regular intervals, the suspension

25

was sampled for MO concentration analysis, which was done by the same means as mentioned in foregoing adsorption section. The percentage of MO absorb was calculated according to the following expression:

$$Absorbance\% = \frac{MO_i - MO_f - MO_{thesolidphotocatalyst}}{MO_i}$$

Eq.2

The absorption of MO will be recorded using UV-vis spectrometer. If the optical absorption edge of the sample shows an appreciable shift toward the visible light region after the doping, therefore, the band gap of the sample can be calculated from the intercept of UV-Vis spectra using the following equation:

$$Eg = \frac{1240}{\lambda}$$

Eq.3

where λ, is the wavelength of the absorption edge in the spectrum (nm).

CHAPTER 4

RESULTS AND DISCUSSION

4.1 Phase identification

TiO_2-Al_2O_3-CNT nanocomposite has been characterized using X-ray diffraction to determine their crystallinity. The XRD patterns of TiO_2-Al_2O_3-CNT nanocomposite were presented in the Figure 4.1. The main peaks which visible in all patterns are at 2θ which equal to 25.562º, 48.037º and 53.884º and it could be identified as anatase TiO_2.

Furthermore, in all patterns there are no new peak either rutile or brookite were formed except for TiO_2 and Al_2O_3. However, there are changes in TiO_2 structure that could be detected with increasing TiO_2 composition. In XRD peak, the peak will be shift either to the left or to the right represent the matrix lattice changes in the nanocomposites. In this case, increasing the composition of TiO_2 and hydrothermal at 200ºC promotes alteration of TiO_2 lattice. Furthermore, there is no significant broadening of all peak patterns could be observed. Thus, increasing TiO_2 content in nanocomposite will decreased the crystallinity of TiO_2 which was later affected the absorption of MO dye (Cheng *et al*., 2012).

Moreover, there is no appearance of CNT peak, this is due to the CNT character which it has small atomic number, therefore, the CNT is hardly been resolved by XRD (Lim., 2014). Besides, this is also due to the solid solution of the Al_2O_3 which has made the CNT diffused into it as the result, thus, the CNT peak cannot be read by the XRD.

27
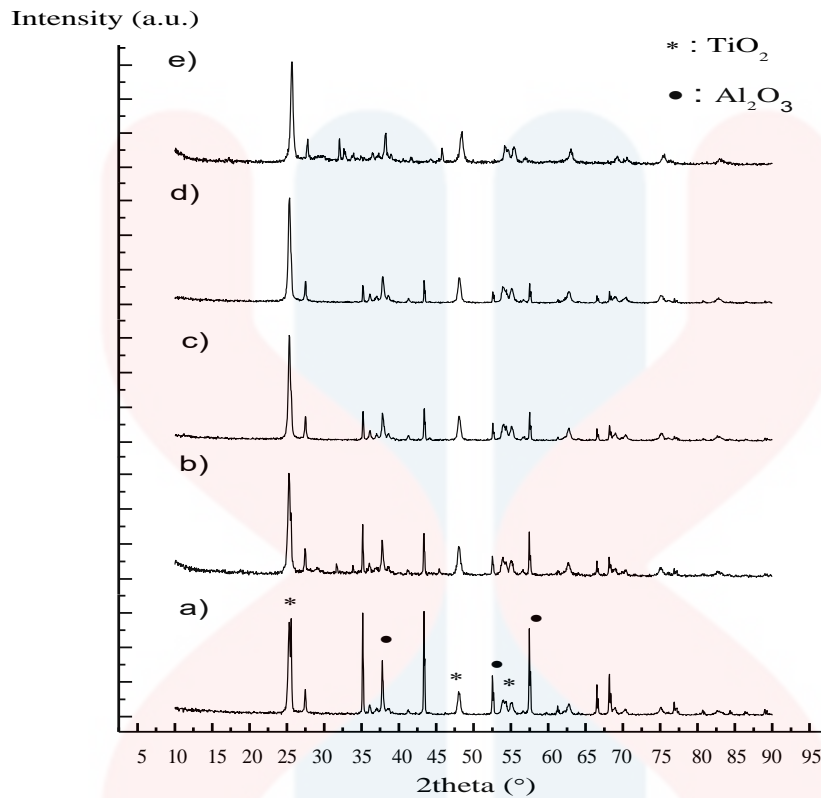
Figure 4.1: XRD pattern of TiO_2 - Al_2O_3 - carbon nanotube nanocomposite with different

compositions a) TA50, b) TAC60, c) TAC70, d) TAC80 and e) TAC90

4.2 Crystallite size and internal grain

In order to calculate the crystallite size and internal strain for the TiO_2-Al_2O_3-CNT nanocomposite the Williamson-Hall method was used. This method is also used to plot the graph illustrates in Figure 4.2. Moreover, the straight line is drawn and having a positive slope. Besides, the broadening peak is at the (-1 0 -1) and (-2 0 0) and the figure show that the crystallite size increases as the internal strain is increased.
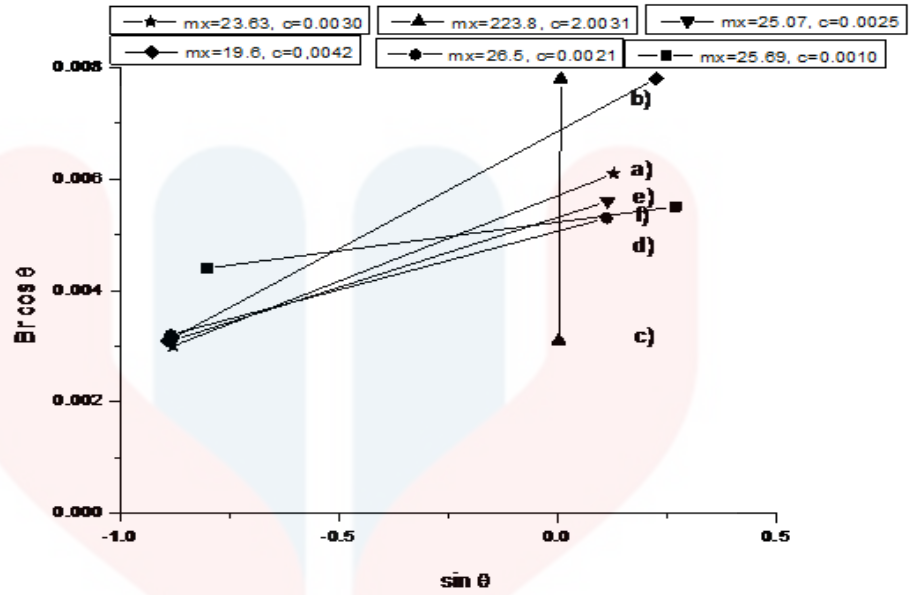
Figure 4.2: Crystallite size and internal grain for TiO_2-Al_2O_3-Carbon nanotube nanocomposite a)

T100, b) TA50, c) TAC60, d) TAC70, e)TAC80 and f) TAC90

Table 4.1: Crystallite size and internal strain for TiO_2-Al_2O_3-Carbon nanotube nanocomposite

Sample	Crystallite size <D>	Internal strain
T100	23.63	0.0030
TA50	19.6	0.0042
TAC60	223.8	2.0031
TAC70	26.5	0.0021
TAC80	25.07	0.0025
TAC90	25.69	0.0010

4.3 Morphology of TiO$_2$-Al$_2$O$_3$-CNT nanocomposite

The optical microscope images of the TiO$_2$-Al$_2$O$_3$-CNT nanocomposites which have been synthesized under different compositions of TA50, TAC60, TAC70, TAC80 and TAC90 samples at the temperature of 200ºC for 24 hours have been illustrates in the Figure 4.3. Therefore, the differences in the morphologies of the samples have been observed. Besides, the combinations of nanotubes ratio structures were produced under the differs composition. Furthermore, according to Wang *et al*., (2013), for TiO$_2$-CNx nanocomposite, its states that on the surface of the CNx, there are TiO$_2$ nanoparticles deposited on it uniformly. Therefore, if the composition of the TiO$_2$ ratio is more compared to Al$_2$O$_3$ and CNT, then, more nanoparticles is visible under the microscope as we observed. Moreover, the compositions is also one of the critical factor in the synthesis of the TiO$_2$-Al$_2$O$_3$-CNT nanocomposite through the oven-assisted hydrothermal method.
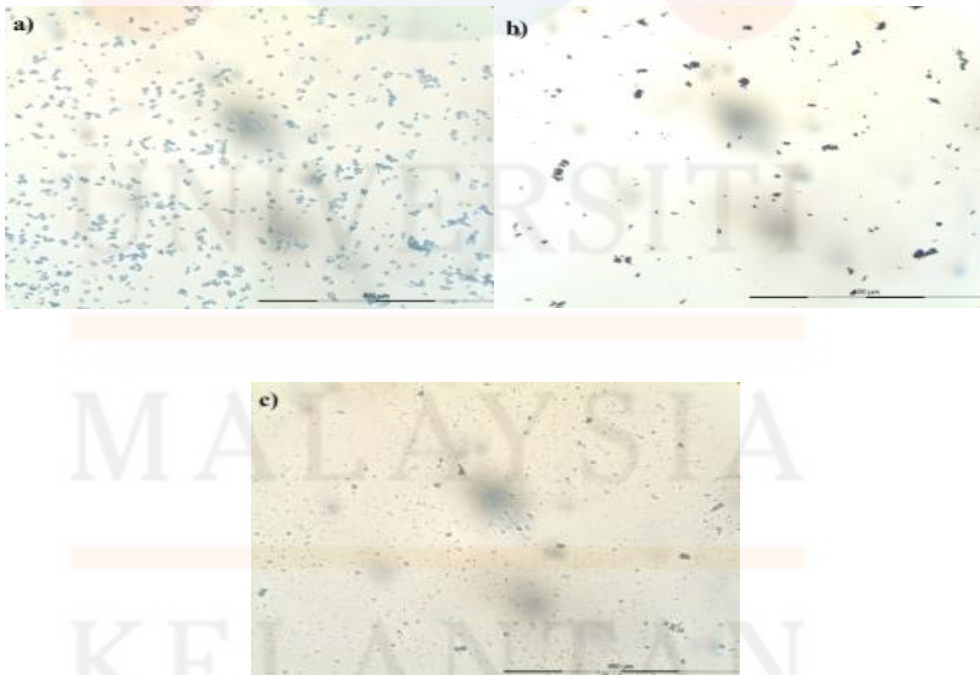
Figure 4.3: Morphology of pure TiO$_2$, Al$_2$O$_3$ and CNT: a) Al$_2$O$_3$, b) CNT and c) TiO$_2$.
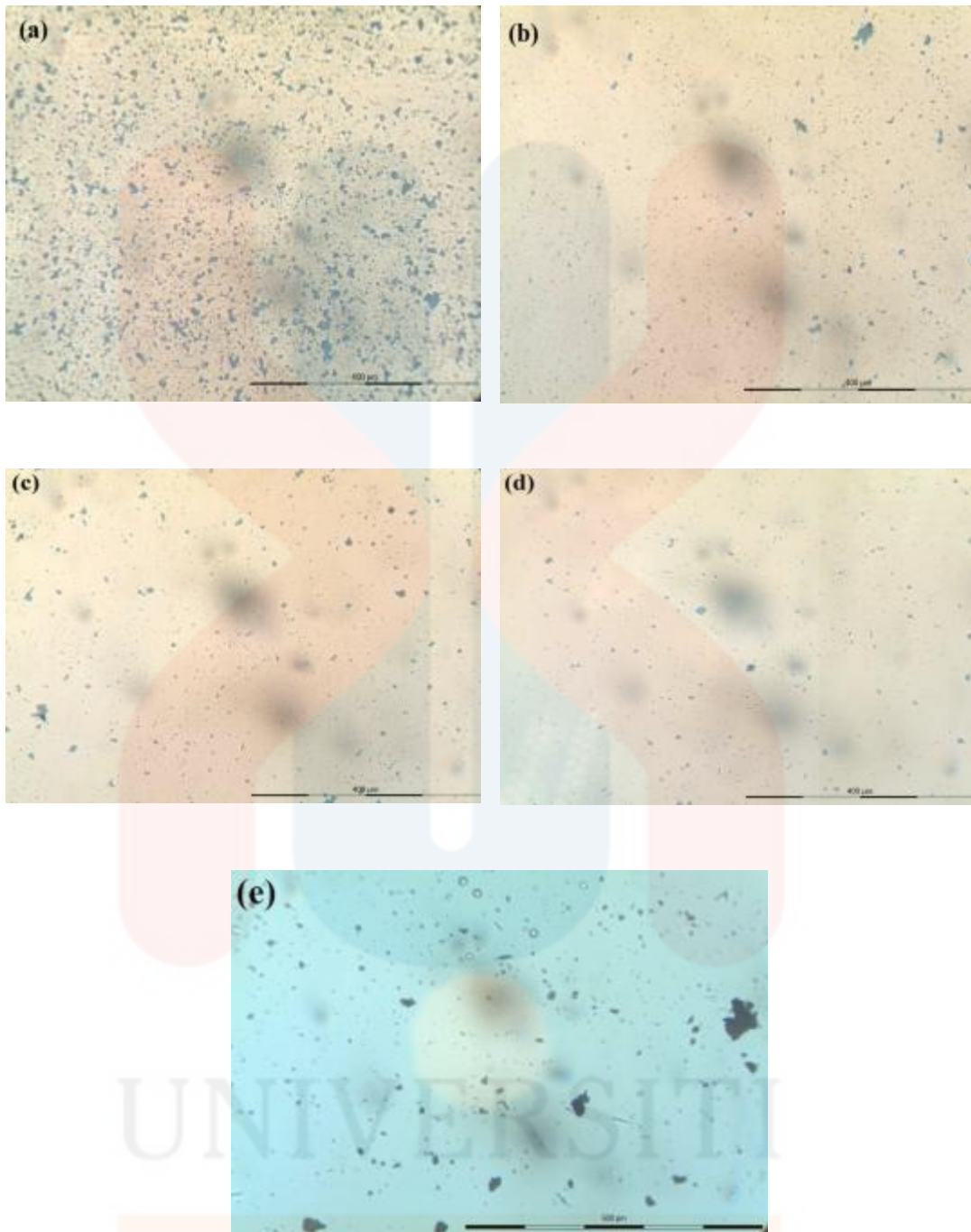
Figure 4.4: Morphology of TiO$_2$-Al$_2$O$_3$-CNT nanocomposite (a) TA50, (b) TAC60, (c) TAC70, (d) TAC80 and (e) TAC90

4.4 Functional group

TiO$_2$-Al$_2$O$_3$-CNT nanocomposite have been characterized using infrared spectroscopy in order to determined their functional group. The FTIR spectra of the

31

obtained sample of TiO_2-Al_2O_3-CNT nanocomposite is shown in Figure 4.5. The figure shows that the strong and broad bands of the infrared spectra is located around the 3000-3500 cm^{-1} where the OH bond is stretching and the H_2O molecules is undergo the vibrational bending. The band spectra that located at 3000-3500 cm^{-1} have been interpret and the result shows that the functional group is the primary aliphatic alcohols. Michele Sherban-Kline (1999) has stated that the alcohols of the hydroxyl group was forms in the spectra and it is due to where the O-H bond is stretching with addition to the C-O bond which was also stretching.

Moreover, the C-O bond that existed in the alcohols of the band spectra is stretching and vibrate and it is due to many other complex absorption that may happen when conducting the experiment. Therefore, the hydroxyl group will be well performed when the O-H bond is stretching compared to when the C-O bond was stretching. Besides, Figure 4.5 also interprets that there are primary aliphatic alcohol of the infrared spectra located around 1000-1100 cm^{-1} and Michele Sherban-Kline (1999) has stated if there are many O-H bond stretch at the lower frequencies, its shows that the hydrogen bond are stronger.

According to Michele Sherban-Kline (1999), the "free" hydroxyl group of the alcohols absorb the spectra strongly at the 3600 cm^{-1} in their vapor phase or dilute solution in non-polar solvents. However, Figure 4.5 shows that the band appear around the 3200-3500 cm^{-1}, this is happening due to the compositions of the sample as it will increase the intermolecular hydogen bonding. Thus, the "free" hydroxyl band for the sample would also be decreases.

In addition, the spectra that occured at 1000-1100 cm^{-1} as shown in Figure 4.5 could be represented as C-O bond if the alcohol is not bonded to the hydrogen and

the absorption number also will be increase.the C-O bonding is strong and it also has been characterized as the C-O bond is stretching.

Figure 4.5 also illustrates the functional group of the band spectra that is located in between 3100-3500 cm^{-1} are aliphatic primary amide. Thus, it shows two ponit. Therefore, for the primary amide, they consist of two N-H bond where the bond is stretching and bending as there are two band which are unsubstituted. Moreover, there are also amide group where the peak is located around 1500-1700 cm^{-1}. It shows that the N-H bond which located there is bending. Furthermore, this peak also will be mistaken for C=C if the corresponding N-H bond is not located at 3200-3500 cm^{-1}.
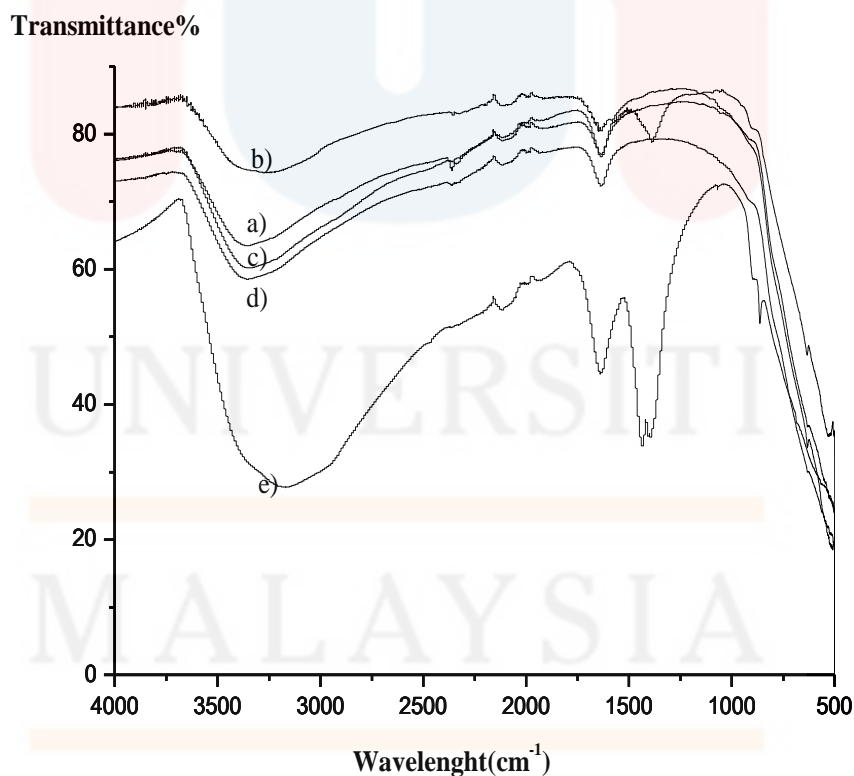
Figure 4.5: FTIR spectra of TiO$_2$-Al$_2$O$_3$-carbon nanotube nanocomposite a) TA50, b) TAC60, c) TAC70, d) TAC80 and e) TAC90

33

4.5 Photocatalytic activity of methyl orange

The TiO_2-Al_2O_3-CNT nanocomposite has been characterized using UV-Vis spectrometer in order to measure the percentage of the methyl orange that has been absorbs. Photocatalytic activity of methyl orange has been conducted for three hours. According to Pecci, (2009) and Anwar, (2015), it stated that the photodegradation of cationic dye optimum under alkaline conditions, this is also due to the ease of formation of the OH radicals on the surface of the photocatalyst TiO_2. Figure 4.6 shows that the light absorption of TiO_2-Al_2O_3-CNT nanocomposite exhibited an increasing absorption in the visible range which is more than 400 nm with an increasing of TiO_2 content.

Moreover, the color of methyl orange is slowly degraded can be seen as there is an increase in the light absorption. Furthermore, it is also favorable as it is a critical factor for the photocatalytic activity. Besides, photocatalytic absorbance reaction of methyl orange was performed with irradiation of visible light. TiO_2-Al_2O_3-CNT is acting as the photocatalyst that could degrade the methyl orange after absorbing the photon energy (hv) which has been provided by the visible light. Thus, the percentage of the absorbance with the light irradiation is much higher than without the irradiation.

Anwar, (2015) has stated that in the dark conditions, TiO_2 was able to act as the absorbance. Therefore, if there is absoption occurs in the dark irradiation, then, it must be due to the characteristic of the TiO_2 as the ratio of TiO_2 is more compared to Al_2O_3 and CNT compositions.
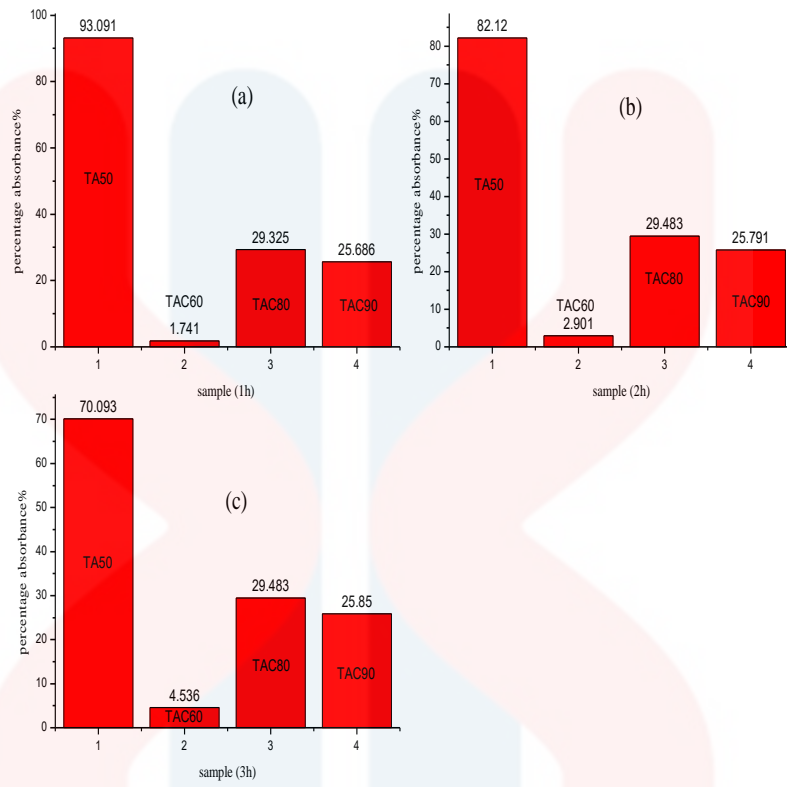
Figure 4.6: Absorbance of TiO$_2$ - Al$_2$O$_3$ - CNT nanocomposite at different time a) 1 h, b) 2 h and c) 3h

CHAPTER 5

CONCLUSION

5.1 Conclusion

In this study, we have synthesized the TiO_2-Al_2O_3-CNT nanocomposite through the hydrothermal method in 200ºC for 24 hours. The conclusions were drawn from the XRD peaks, FTIR functional group, Optical microscope for the morphologies and the photocatalytic activity are stated as below:

1. TiO_2 structure was altered with the addition of Al_2O_3 and CNT .

2. The functional group that found in TiO_2- Al_2O_3-CNT nanocomposite were alcohol and amide group.

3. Morphology of the nanocomposite showed agglomerated particles of TiO_2, Al_2O_3 and CNT particles.

4. Nanocomposite with no addition of CNT showed the highest absorbance of methyl orange.

5.2 Recommendations

In order to characterize the TiO_2-Al_2O_3-CNT nanocomposite the parameter such as temperature should have been investigated further. Besides, the presence of others materials and the grain of the morphologies of the sample cannot be seen, so the study using SEM or TEM machine could help us to explore more on the difference morphologies that appeared under the microscope.

REFERENCES

Anwar D.I. & Mulyadi D. (2015). Synthesis of TiO_2 Composite as a Photocatalyst for Degradation of Methylene Blue. *Procedia Chemistry, 17,* 49-54.

Bagheri S., Hir Z. A. M., Termeh A. T. & Hamid S. B. A. (2015). Progress on mesoporous titanium dioxide: Synthesis, modification and applications. *Microporous and mesoporous materials, 218*, 206-222.

Davis K. (2010). Material Review: Alumina (Al_2O_3). *School of Doctoral Studies (European Union) Journal, 2010,* 109-114.

Chang B. Y., Huang N. M., An'amt M. N., Marlinda A. R., Norazriena Y., Muhamad M. R., Harrison I., Lim H. N. & Chia H.C. (2012). Facile hydrothermal preparation of titanium dioxide decorated reduced graphene oxide nanocomposite. *Int J Nanomedicine, 7*, 3379-3387.

Cividanes L.S., Simonetti E.A.N., Moraes M.B., FernandesF.W. & Thim G.P. (2014). Influence of carbon nanotubes on epoxy resin cure reaction using different techniques: A comprehensive review. *Polymer Engineering & Science, 54*(11), 2461-2469.

Estili M. & Sakka Y. (2014). Recent advances in understanding the reinforcing ability and mechanism of carbon nanotubes in ceramic matrix composites. *Science and Technology of Advanced Materials,15(6),*

Ezeigwe E.R., Tan M.T.T., Khiew P.S. & Siong C.W. (2015). Solvothermal synthesis of graphene–MnO2 nanocomposites and their electrochemical behavior. *Ceramics International, 41*(9), 11418-11427.1468-6996.

Flores I.C., De Freitas J.N., Longo C., Paoli M.A.D., Winnischofer H. & Nogueira A.F. (2007). Dye-sensitized solar cells based on TiO2 nanotubes and a solid-state electrolyte. *Journal of Photochemistry and Photobiology A: Chemistry, 189*(2-3), 153-160.

Gutierrez-Gonzaleza C.F., Smirnov A., Centeno A., Fernández A., Alonso B., RochaV,G., Torrecillas R., Zurutuza A. & Bartolome J.F. (2015). Wear behavior of graphene/alumina composite. *Ceramics International, 41(6),* 7434-7438.

Hussain S. T., & Siddiqa A. (2011). Iron and chromium doped titanium dioxide nanotubes for the degradation of environmental and industrial pollutants, *Int. J. Environ. Sci. Tech, 8(2),* 351-362.

Jiang F., Zheng S., Ana L. & Chen H. (2012). Effect of calcination temperature on the adsorption and photocatalytic activity of hydrothermally synthesized TiO_2 nanotubes. *Applied Surface Science, 258,* 7188-7194.

Khalid N. R., Ahmed E., Hong Z., Zhang Y. & Ahmad M. (2012). Nitrogen doped TiO$_2$ nanoparticles decorated on graphene sheets for photocatalysis applications. *Current Applied Physics, 12*(6), 1485-1492.

Leary R. & Westwood A. (2011). Carbonaceous nanomaterials for the enhancement of TiO$_2$ photocatalysis. *Carbon 49, 2011,* 741-772.

Liu N., Chen X., Zhang J. & Schwank J.W. (2014). A review on TiO$_2$-based nanotubes synthesizedvia hydrothermal method: Formation mechanism, structure modification, and photocatalytic applications. *Catalysis Today, 225,* 34-51.

Long X., Bai Y., Algarni M., Choi Y. & Chen Q. (2015). Study on the strengthening mechanisms of Cu/CNT nano-composites. *Materials Science & Engineering A, 645,* 347-356.

Nursam N.M., Wang X. & Caruso R.A. (2015). High-Throughput Synthesis and Screening of Titania-Based Photocatalysts. *ACS Combinatorial Science, 17(10),* 548-569.

Park H., Park Y., Kim W. & Choi W. (2013). Surface modification of TiO2 photocatalyst for environmental applications. *Journal of Photochemistry and Photobiology C: Photochemistry Review, 15,* 1-20.

Pei J., Ma W., Li R., Li Y. & Du H. (2015). Preparation and Photocatalytic Properties TiO$_2$-Al$_2$O$_3$ Composite Loaded Catalyst. *Hindawi Publishing Corporation Journal of Chemistry, 2015,* 7.

Poliah R. & Sreekantan S. (2011). Characterization and Photocatalytic Activity of Enhanced Copper-Silica-Loaded Titania Prepared via Hydrothermal Method. *Hindawi Publishing Corporation Journal of Nanomaterials, 2011,* 8.

Qamar M., Yoon C.R., Oh H.J., Lee N.H., Park K., KimD.H., Lee K.S., Lee W.J. & Kim S.J. (2008). Preparation and photocatalytic activity of nanotubes obtained from titanium dioxide. *Catalysis Today, 131*(1-4), 3-14.

Sarkar S. & Das P. K. (2014). Effect of sintering temperature and nanotube concentration on microstructure and properties of carbon nanotube/alumina nanocomposites. *Ceramics International, 40(5),* 7449-7458.

Sekabira K., Origa H.O., Basamba A., Mutumba G. & Kakudidi E. (2010). Heavy metal assessment and water quality values in urban stream and rain water. *Int. J. Environ. Sci. Tech., 7* ((4)), 759-770.

Simões S., Viana F., Reis M.A.L. & Vieira M.F. (2015). Influence of dispersion/mixture time on mechanical properties of Al–CNTs nanocomposites. *Composite Structures, 126,* 114-122.

Su C., Tseng C.M., Chen L.F., You B.H., Hsu B.C. & Chen S.S. (2006). Sol–hydrothermal preparation and photocatalysis of titanium dioxide. *Thin Solid Films, 498(1),* 259-265.

Sun H., Wang H., Ang H.M., Tadé M.O. & Li Q. (2010). Halogen element modified titanium dioxide for visible light photocatalysis. *Chemical Engineering Journal, 162*(2), 437-447.

Thomson K.E., Jiang D., Yao W., Ritchie R.O. & Mukherjee A.K. (2012). Characterization and mechanical testing of alumina-based nanocomposites reinforced with niobium and/or carbon nanotubes fabricated by spark plasma sintering. *Acta Materialia, 60,* 622-632.

Trunec M., Maca K. & Chmelik R. (2015). Polycrystalline alumina ceramics doped with nanoparticles for increased transparency. *Journal of the European Ceramic Society, 35(5),* 1001-1009.

APPENDICES

A.1 Pphotocatalytic activity of Methyl Orange (MO)
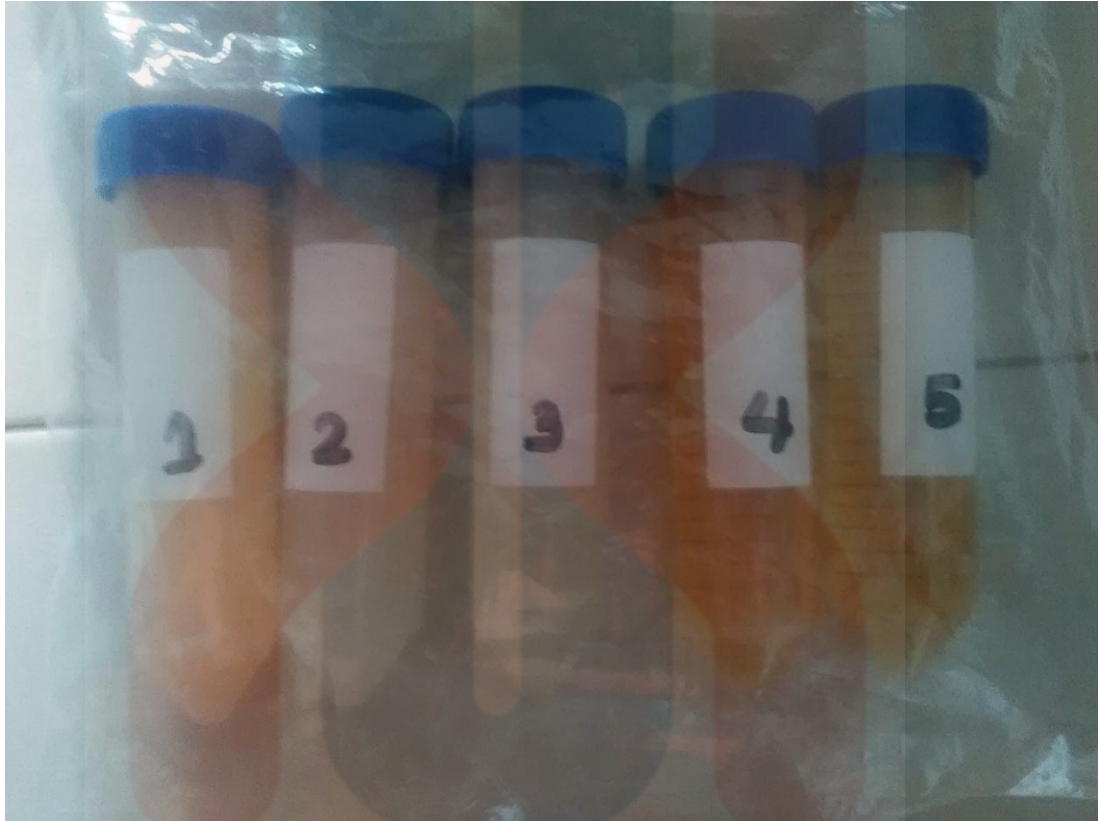
A.2 Williamson Hall methods

Sample No	hkl	2θ(Obs.Max)	θ	cosθ	B(°)	B (rad)	B_i(°)	B_i (rad)	$B_r^2 = B^2 - B_i^2$	$B_r cosθ$	sinθ	<D>	Strain
T100	1 0 -1	25.391	12.6955	0.9916744	0.364	0.0064	0.1	0.0017	0.0061	0.0061	0.1287708	0.0057	0.0030
	2 0 0	48.116	24.058	0.4759598	0.378	0.0066	0.1	0.0017	0.0064	0.0030	-0.879467	2.363E-08	0.1503
Sample No	hkl	2θ(Obs.Max)	θ	cosθ	B(°)	B (rad)	B_i(°)	B_i (rad)	$B_r^2 = B^2 - B_i^2$	$B_r cosθ$	sinθ	<D>	Strain
TA50	1 0 -1	25.585	12.7925	0.9745415	0.468	0.0082	0.1	0.0017	0.0080	0.0078	0.2242071	0.0068	0.0042
	2 0 0	48.068	24.034	0.4547176	0.405	0.0071	0.1	0.0017	0.0069	0.0031	-0.890636	1.96E-08	0.2091
Sample No	hkl	2θ(Obs.Max)	θ	cosθ	B(°)	B (rad)	B_i(°)	B_i (rad)	$B_r^2 = B^2 - B_i^2$	$B_r cosθ$	sinθ	<D>	Strain
TAC60	1 0 -1	25.316	12.658	0.995805	0.461	0.0080	0.1	0.0017	0.0079	0.0078	0.0036	0.0006	2.0031
	2 0 0	48.063	24.0315	0.4524896	0.402	0.0070	0.1	0.0017	0.0068	0.0031	0.0012	2.238E-07	100.1557
Sample No	hkl	2θ(Obs.Max)	θ	cosθ	B(°)	B (rad)	B_i(°)	B_i (rad)	$B_r^2 = B^2 - B_i^2$	$B_r cosθ$	sinθ	<D>	Strain
TAC70	1 0 -1	25.356	12.678	0.9937759	0.321	0.0056	0.1	0.0017	0.0053	0.0053	0.1113977	0.0051	0.0021
	2 0 0	48.097	24.0485	0.4675836	0.406	0.0071	0.1	0.0017	0.0069	0.0032	-0.883949	2.65E-08	0.1045
Sample No	hkl	2θ(Obs.Max)	θ	cosθ	B(°)	B (rad)	B_i(°)	B_i (rad)	$B_r^2 = B^2 - B_i^2$	$B_r cosθ$	sinθ	<D>	Strain
TAC80	1 0 -1	25.362	12.681	0.9934372	0.34	0.0059	0.1	0.0017	0.0057	0.0056	0.1143785	0.0053	0.0025
	2 0 0	48.117	24.0585	0.4763995	0.389	0.0068	0.1	0.0017	0.0066	0.0031	-0.879229	2.507E-08	0.1263
Sample No	hkl	2θ(Obs.Max)	θ	cosθ	B(°)	B (rad)	B_i(°)	B_i (rad)	$B_r^2 = B^2 - B_i^2$	$B_r cosθ$	sinθ	<D>	Strain
TAC90	1 0 -1	25.678	12.839	0.9630662	0.341	0.0060	0.1	0.0017	0.0057	0.0055	0.2692646	0.0052	0.0010
	2 0 0	48.407	24.2035	0.5984421	0.436	0.0076	0.1	0.0017	0.0074	0.0044	-0.801166	2.569E-08	0.0489